



Research paper

Estimation of the transfer number, B using biomass sphere combustion with initial temperature variation

A. Shivakumar*, Sachin Payyanad, H.S. Mukunda, C.S. Bhaskar Dixit

Fire & Combustion Research Center, Jain (deemed to be) University, Kanakapura Road, Bangalore, India

ARTICLE INFO

Keywords:

Burn rate
Biomass
Modelling
Initial temperature effect
Heat of pyrolysis
Transfer number

ABSTRACT

Studies have been conducted on the mass burn rate of spheres with six different species of 10, 15, and 20 mm diameter, with some species at various initial temperatures namely, 300, 373, 393 and 423 K (that are below pyrolysis conditions) to examine the possibility of determining the heat of pyrolysis and so the transfer number, B for biomass species. Ficus, Pine, Acacia, Ivory, Tamarind, and Balsa with density variation from 250 to 950 kg/m³ and at moisture fractions of 0 to 0.12, with four of them at different initial temperatures were experimentally studied to help determine the constants in a burn rate correlation developed using scaling laws. In respect of the initial temperature effect, the increase in the mass burn rate is up to 25% and in respect of increase in moisture fraction, the mass burn rate decrease is by a maximum of 25%. The data of more than 90 experiments are used in a model based on scaling laws to extract the heat of pyrolysis and so, the transfer number, B and match the mass burn rate data. The key parameter affecting B is the heat of pyrolysis (or phase change) that is taken to be different for different species. Experiments and analysis lead to the determination of both H_{p0} , the parameter connected to the heat of pyrolysis and B . Most species show endothermic values of the heat of pyrolysis and the value of B varies from 0.8 to 1.8 over the biomass tested and the burn rate predictions from the model compare with experiments to within a mean square error of 5%. A procedure for determining the transfer number for any given biomass has been presented.

1. Introduction

Three motivations have led to the extensive study of thermochemical conversion of biomass. When used as a source of energy, the design of the gasification or combustion system requires an understanding the burn behaviour as influenced by its density, shape, size and moisture effects (Ragland and Aerts [1], Huff [2]). When used as an infrastructure in buildings, the interest is to see how to avoid unintended fires or minimize the ill-effect due to one of the parameters as above, noting that there is no control on the choice since they are already fixed in the infrastructure (Friquin [3]). The third motivation is to study product distribution in pyrolytic conditions to enable obtain biochar of a desired specification (Maa and Baille [4]; Pyle and Zaror [5]; de Blasi [6]). In the first one, enhancement of combustion is achieved through the use of forced convection of air. In the second one, estimates have to be made of the heat transfer by radiation from adjoining fires or heated surfaces and the heat release of reacting pyrolysed solid material with air induced by free convection. In the third one, detailed chemical and structural analysis are performed on relatively small samples using radiant heat flux

and track the product distribution. The condensed phase processes are similar. Heat absorption by conduction to a temperature at which condition pyrolysis becomes significant is a key feature. The heating rates are large in the case of combustion process. The heating rates in the case of fires vary from small to large and simulation of this is performed through the use of radiant sources like in a cone calorimeter. In the third case, the radiation flux is set as a part of the experiment. Studies on the fundamentals of the process – combustion or fire – have been made for over six decades. In understanding and modelling of all the thermochemical conversion processes, Spalding's transfer number, B which is the ratio of the gas phase enthalpy difference to that in the condensed phase is an important parameter identified with individual liquid fuels. In books on combustion (see for instance, p. 262+, Glassman [7]), B is invoked in all phase transition problems. However, literature is largely silent on the value of B for biomass fuels even though the variation in the thermal properties is wide. The aim of the present work is to examine the issue and evolve a procedure to determine the transfer number specific to a biomass fuel and in doing so, determine its value for a select group of six fuels.

* Corresponding author.

E-mail address: shivakumarannaiappa@gmail.com (A. Shivakumar).

2. Earlier work

Experiments on the burn behaviour of wood of cubical and rectangular geometries have been made by some researchers. Bartlett et al. [8] in their review of the burning behaviour of wood have described all the phases of the combustion process and have provided the data from earlier work. Observations on the burn rate effects of density and moisture from the data suggest a possible overlap, a feature remedied by Friquin [3] as he brought out the density effects on charring rates under irradiated conditions. Tinney [9], Capart et al. [10], de Ris et al. [11] have examined pyrolysis and combustion behaviour of cylinders of wood at ambient and higher pressures with and without flow of nitrogen or depending on whether pyrolysis or combustion is to be simulated. Maa and Bailie [4] have conducted a modelling study delineating the regimes of diffusion dominated and reaction dominated behaviour. Increase in sample radius beyond 30 mm is stated to be diffusion controlled and less than 1 mm reaction controlled. The intermediate regime is covered by the combined role of both chemical kinetics and diffusion. Lu et al. [12,13] have presented a study of the combustion of single particles.

Blackshear and Murty [14] performed experiments on cylindrical cellulosic samples and measured the mass loss and temperatures of samples at various radii. The measured temperature time histories with the DTA values were interpreted to infer that the decomposition of the samples takes place endothermically at temperatures of 573–673 K and exothermically above 773 K. Also, they have tried to extract the mass transfer number B for the solid fuel by deploying the method similar to that for methanol fuel and inferred its value as 1.5. Orloff and de Ris [15] also remark that the transfer number of biomass as 1.5 without any qualifying observations. The transfer number is defined as follows:

$$B = \frac{c_{pg}(T_f - T_s)}{[H_p + c_{pf}(T_s - T_{ini})]} \quad (1)$$

where c_{pg} is the gas phase specific heat, T_f and T_s are the flame (or gas phase) and surface temperatures, H_p is the heat of pyrolysis, c_{pf} is the specific heat of the fuel and T_{ini} is the initial fuel temperature. Just as for liquid fuels where these properties depend on the specific fuel, it should be expected that these values should depend on the specific biomass and the value of $B = 1.5$ can at best be treated as an indicative value. Two key parameters, c_{pf} and H_p that affect B have been explored in the literature. Ragland and Aertis [1] have presented the broad parameters for several thermal properties based on earlier data. Specific heat increases with initial temperature and moisture content with values varying from 1.3 to about 2 kJ/kg K. More recent studies by DuPont et al. [16] have shown that the specific heat is nearly the same for more than 20 species that they studied and hence confirmed the conclusions of Ragland and Aertis [1]. Also, Radmanovic et al. [17] have presented a review indicating similar results over a different range of biomass.

In so far as heat of pyrolysis is concerned, there has been much debate in the literature. Roberts [18,19] has indicated the issues related to H_p . A discussion on the paper (Roberts [18]) by Kanury Murty keeps the matter related to exothermicity or otherwise of the pyrolysis process unsettled. Later, Milosavljevic et al. [20] have summarized the values of H_p by different researchers over a time and the range of values is from -2100 kJ/kg to $+2500$ kJ/kg on the basis of mass of volatiles, the negative sign representing exothermicity. The results from several researchers have been re-examined by others providing qualitatively different values for the heat of pyrolysis. For instance, the reported values of Roberts and Clough [21] as -314 to -1700 kJ/kg has been modified by Kung and Kalekar [22] using a more refined calculation procedure as $+203$ kJ/kg. What is more, the basis of most of these results is the amount of volatiles which in itself is another parameter that could vary between 0.5 to 0.8 of the mass of the solid fuel depending essentially on the heating rate adopted in the studies. As

such, one can recognize that the uncertainty in the values of H_p arising out of these studies is wide.

One classical argument that since the burn rate, \dot{m} depends on B through $\ln(1 + B)$, larger changes in B will not influence the estimate of burn rate significantly leaves the question of determination of B for biomass uninteresting for resolution and therefore the question has remained open. We can estimate the sensible enthalpy of the biomass as it heats up from 300 K up to the pyrolysis temperature, say, 600 K for the choice of c_{pf} of 1.5 kJ/kg K as 450 kJ/kg. If the gas phase enthalpy change = $c_{pg}(T_f - T_s)$ which is the numerator in the equation for B is estimated as $= 1 \times (1300 - 600) = 700$ kJ/kg and the transfer number, B is taken as 1.5, the value of H_p will have to be $+16$ kJ/kg (endothermic). This range appears small considering the range of values set out in Milosavljevic et al. [20]. If the value of H_p is say 100 kJ/kg, $B = 1.27$ and if it is -100 kJ/kg, $B = 2$. The change in burn rate which is proportional to $\ln(1 + B)$ will be by a factor of 1.34 between the H_p values of -100 to 100 kJ/kg. This change is not small considering the fact that the H_p values have a wide range of uncertainty.

Roberts [18] presented arguments indicating that the process of pyrolysis in wood can be understood to be composed of that of its constituents — largely of cellulose and lignin with cellulose showing much smaller exothermicity than lignin. Additional arguments are made to indicate that the structure of wood also has influence on the heat of pyrolysis. What appears as a significant outcome of this work is that the biomass composition that would include extractives and crude protein can all influence the pyrolysis process. This allows for the possibility of the value of B for biomass to be dependent on the composition even if such a dependence may not be very strong.

A few studies have been completed on the combustion of cubes and spheres of biomass. Huff [2] conducted experiments on cubes 5 mm to 20 mm in size made of balsa, pine, and oak. The process is conducted in a furnace maintained at various test temperatures, 797, 1963, and 1345 K. The plot of the burn time as a function of the size is the test data. Because the experiments have heat transfer from the furnace also and also the process of ignition of larger size cubes can take time, the data reduction to derive fundamental information requires further analysis. Kuo and Hwang [23] conducted experiments with rosewood spheres of 20 mm and 50 mm diameter in air streams at 673 and 773 K at Reynolds numbers of 250 to 1000. The process of ignition was tracked and related to in-depth conduction parameters. The burn rate data from these studies seem so deeply connected to the ignition process that the starting condition for combustion is different for various cases making it difficult to draw more fundamental inferences. For instance, for the same 20 mm diameter sphere at the same furnace temperature of 773 K, the samples are ignited by the flow of hot air and so, the combustion process is coupled with the ignition process which varies with the Reynolds number. For instance, the burn flux changes from 8.6 to 10.7 g/m²s with change in Reynolds number from 208 to 346. The sample undergoing combustion at 773 K is at different levels preparation in terms of loss of volatiles and hence the combustion process cannot be treated identical. Nevertheless, the observed maximum burn flux obtained around the point of ignition or the beginning of flaming combustion is in the range of 10 to 18 g/m²s depending on the size of wood sphere and heating conditions.

Mukunda et al. [24] conducted experiments on teak wood spheres, 10 to 25 mm diameter and stated a result for the burn rate as follows.

$$\dot{m} = 7 \times 10^{-4} d_s \quad (2)$$

with \dot{m} in kg/s and d_s in m. The scaling of mass burn rate with d_s has been brought out from this study. This result can also be expressed for the burn time, t_b as

$$\frac{t_b}{(\rho_{fu}/650)} = 50 \left[\frac{d_s}{10} \right]^2 \quad (3)$$

where the biomass density, ρ_{fu} is in kg/m³ and the diameter of the wood sphere, d_s is in mm. This result is an average behaviour of the

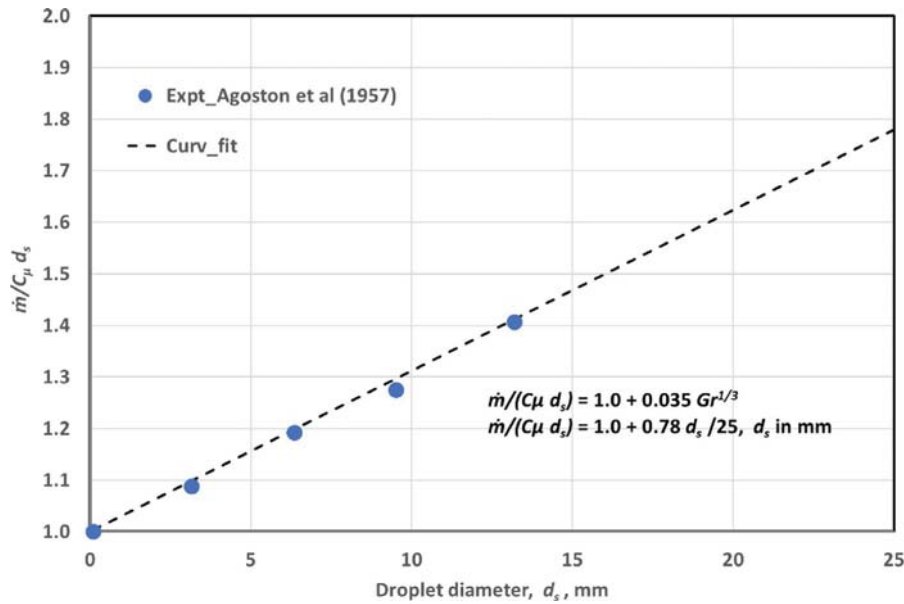


Fig. 1. Experimental results of Agoston et al. [25] and a curve fit.

data since their experimental data show a 30% increase in \dot{m}/d_s with the diameter increasing from 10 to 25 mm. The analysis performed that accounts for free convective transfer using standard correlation based on the experimental data of Agoston et al. [25] shows that increase in \dot{m}/d_s over the diameter range of about 30%. Interestingly, Agoston et al. [25] are the only authors to have done experiments on liquid fuels at large diameters to enable extracting the data for free convective effects. Their work was on spheres of 3.15, 6.35, 9.51 and 13.2 mm diameter (comparable to the size of wood spheres) made of porous alundum that was fed by the liquid fuel by a short, stainless-steel, hypodermic-tubing feed line such that the surface of the sphere is just wet. These results are considered in the present study. Baum and Atreya [26] has performed thermal simulations assuming quasi steady burning on oblate and prolate geometries and presented the results of burn time with mass. All the data collapse on to a single curve which can be interpreted in terms of an equivalent sphere shows that $t_b \sim d_s^{2.15}$. This implies that the process is diffusion limited, a generally known result.

3. The basis of the present approach

In view of the discussion above, it appears that a new approach needs to be developed to estimate B . It is first to be noted that mass burn rate is the most important outcome of such studies and relevant for the design of combustion and fire safety situations. It is considered important to use a simple geometry for tests and analysis.

In order to design experiments to extract B , we start with the basic mass burn rate expression for a fuel sphere as

$$\dot{m}_n = \dot{m}/C_\mu d_s \quad (4)$$

$$= \ln(1+B)f(Gr, Si_d) \quad (5)$$

$$C_\mu = 2\pi(\mu_g/Pr) \quad (6)$$

$$B = c_{pg}(T_f - T_s)/[H_p + c_{pf}(T_s - T_{ini})] \quad (7)$$

where \dot{m}_n is the dimensionless mass burn rate, d_s is the sphere diameter, C_μ is a constant depending on the chosen values of μ_g , the representative gas phase viscosity and the Prandtl number, Pr , $f(Gr, Si_d)$ is the function of Grashof number, Gr to address convective effects and Si_d , the change in diameter of the biomass due to shrinkage during volatilization. The above expression without Si_d is the standard burn

rate expression valid for liquid droplets and also for solid spheres with little change in size.

It was brought out earlier that the denominator of B has $c_{pf}(T_s - T_{ini})$ which is significant, amounting to 450 kJ/kg at T_{ini} of 300 K. The aim is to study how the biomass burn rate varies if T_{ini} is increased to as high values as possible so that the sensible enthalpy part can be reduced. Typically, T_s is about 600 K and various DTA/TGA studies suggest that decomposition begins at around 473 K. Thus, the maximum value of T_{ini} will be 473 K. By conditioning the biomass spheres at various higher temperatures, the condensed phase enthalpy term can be brought down and perhaps, this would increase B . The word *perhaps* is used because it is not clear if H_p remains the same. The approach chosen here is to conduct experiments on the determination of burn characteristics of several species at various conditions that will affect the transfer number B significantly. The parameters under control are the moisture content that is intended to be varied up to sun-dry conditions (up to 12%) on the one side and heat it to obtain 0% moisture at ambient temperature and raise biomass conditioning temperature to 473 K in steps. The process of determining H_p and therefore B would be to seek good comparison of the above model with a wide range of data as wide as possible. More discussion on this follows.

Now we consider the expression related to Gr in the above equation. The Grashof number is defined by

$$Gr = [g(T_f - T_{ini})/T_{ini}]d_s^3/(\mu_g/\rho_g)^2 \quad (8)$$

The choice of values for μ_g and ρ_g are important to obtain predictions without an arbitrary constant. This choice is based on earlier work by Mukunda [27] and Raghunandan and Mukunda [28] where it has been shown that the variation of properties through the diffusion flame is very significant and the better representation of the properties will be those that are close to the flame. For liquid drops, the values of C_μ works out to 7×10^{-4} kg/m s. With other values for the parameters, $g = 9.81$ m/s², $T_f = 1200$ K, $T_{ini} = 300$ K, $\mu_g = 6.6 \times 10^{-5}$ kg/m s, $\rho_g = 0.4$ kg/m³, we get $Gr/d_s^3 = 1.08 \times 10^9$.

Typical enhancement due to free convection is expressed as $(1 + C_0 Gr^n)$. Earlier work by Agoston et al. [29] indicates that $n = 0.3$. The experimental data of Agoston et al. [25] is related to forced convection effects on the burn rate of larger drops. The data can be extrapolated back to zero forced convection to lead to free convection effects. These data are taken from their work and plotted against the drop diameter, d_s . Fig. 1 shows such a plot. The variation is linear with respect to

Table 1

Results of proximate and ultimate analysis on dry basis, all the values are in %, Vole = Volatile, FixC = Fixed carbon.

Species	Proximate analysis			Ultimate analysis				
	Vole	FixC	Ash	C	H	N	O	S
Ficus	82.8	16.3	0.9	50.7	4.8	0.4	43.1	0.1
Ivory	84.5	14.5	1.0	46.9	5.7	1.1	44.9	0.2
Acacia	82.8	16.8	0.4	48.2	4.9	2.2	44.2	0.1
Pine	82.5	17.1	0.4	50.2	4.4	0.6	43.7	0.6
Tamarind	82.1	16.9	1.0	50.1	5.5	0.6	41.3	1.1
Balsa	84.2	14.8	1.0	47.1	4.9	0.9	45.7	0.3

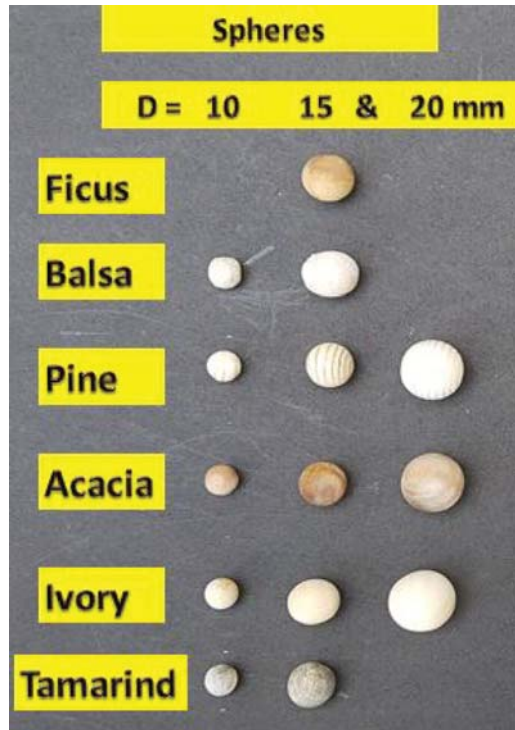


Fig. 2. Samples of different species used in the experiments.

drop diameter indicating that the correction can be expressed as $(1 + C_0 Gr^{1/3})$. The constant C_0 works out to 0.035. The expression can be recast in terms of the diameter of the sphere, normalizing it with a diameter of 25 mm. The resulting correction due to free convection becomes $(1 + 0.78 d_s/25)$ with d_s expressed in mm. With this correction, the expression becomes

$$\dot{m}_n = \ln(1 + B) \left[1 + 0.78 \frac{d_s}{25} \right] f_1(Si_d) \quad (9)$$

We now consider $f_1(Si_d)$, the effect of shrinkage. Much effort seems to have gone into developing detailed models and conducting experiments on the shrinkage effects in pyrolysis under the influence of radiant heat flux, the emphasis being on the product distribution (Barr et al. [30], di Blasi [6], Huang et al. [31]). Since the nature of biomass is very broad, the comparisons between predictions of detailed models and computation coupled with the assumptions of kinetics based on multi-step chemistry have remained quantitatively inadequate. This is so because the condensed phase chemistry is dependent on catalytic effects of inorganic ingredients drawn from the soil at the particular location where the tree is growing apart from inherent differences in the composition of cellulose, lignin and others. Precisely because of these reasons, it is unlikely that quantitative predictions will improve until a long time. Huang et al. [31] have provided some excellent photographic evidence of biomass shrinkage of 20 and 30 mm diameter

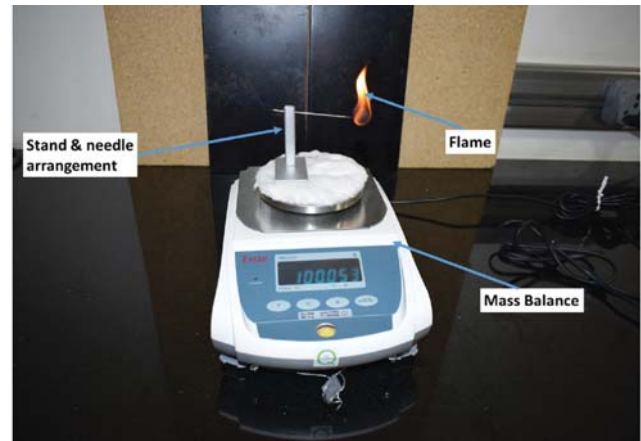


Fig. 3. Schematic of experimental arrangement used in the experiments to obtain mass loss vs time for spheres.

spheres as they undergo thermal pyrolysis at temperatures of 673 to 973 K. Even though the pyrolysis process may not be completely representative of the phenomenon that occurs during combustion, the shrinkage values may actually be within the right order of magnitude. The results show a shrinkage of 12 to 15% for a temperature of 673 K and at a duration of about 200 s typical of flaming combustion times of biomass considered here. The density of biomass (ρ_{fu}) used in this experiment is 560 kg/m^3 . Even though the modelling effort on the biomass shrinkage has been extensive, there are no specific efforts to determine the role of density in the shrinkage process. Experimental evidence on teak wood sphere combustion (Mukunda et al. [24]) which has little dependence on chemistry insofar as burn rate behaviour is concerned shows that by the end of flaming, there is a reduction in diameter of about 10%. Thus we need to describe the shrinkage behaviour during flaming to account for size changes in the burn rate behaviour and the magnitude of the shrinkage being about 10%. The effective mean value of shrinkage over the burn period is perhaps 6 to 7%. The question of which overall parameter controls the shrinkage the most and based on earlier laboratory studies on wood of varying density, initial biomass density has been considered as the critical parameter in affecting the shrinkage with higher density leading to lower shrinkage. The following equation was therefore set out.

$$f_1(Si_d) = 1 - 0.07 (650/\rho_{fu}) \quad (10)$$

where the fraction 0.07 was chosen based on the experimental value for teak with a density of 650 kg/m^3 . Typical densities considered in the present study vary from 250 to 950 kg/m^3 . $f_1(Si_d)$ will vary between 0.82 to 0.95. Even though these values cause changes that are not significantly different from the accuracies of experiments (to within $\pm 5\%$), it was thought appropriate to include as a systematic effect. The mass burn equation will now read as

$$\dot{m}_n = \ln(1 + B) \left[1 + 0.78 \frac{d_s}{25} \right] \left[1 - 0.07 \frac{650}{\rho_{fu}} \right] \quad (11)$$

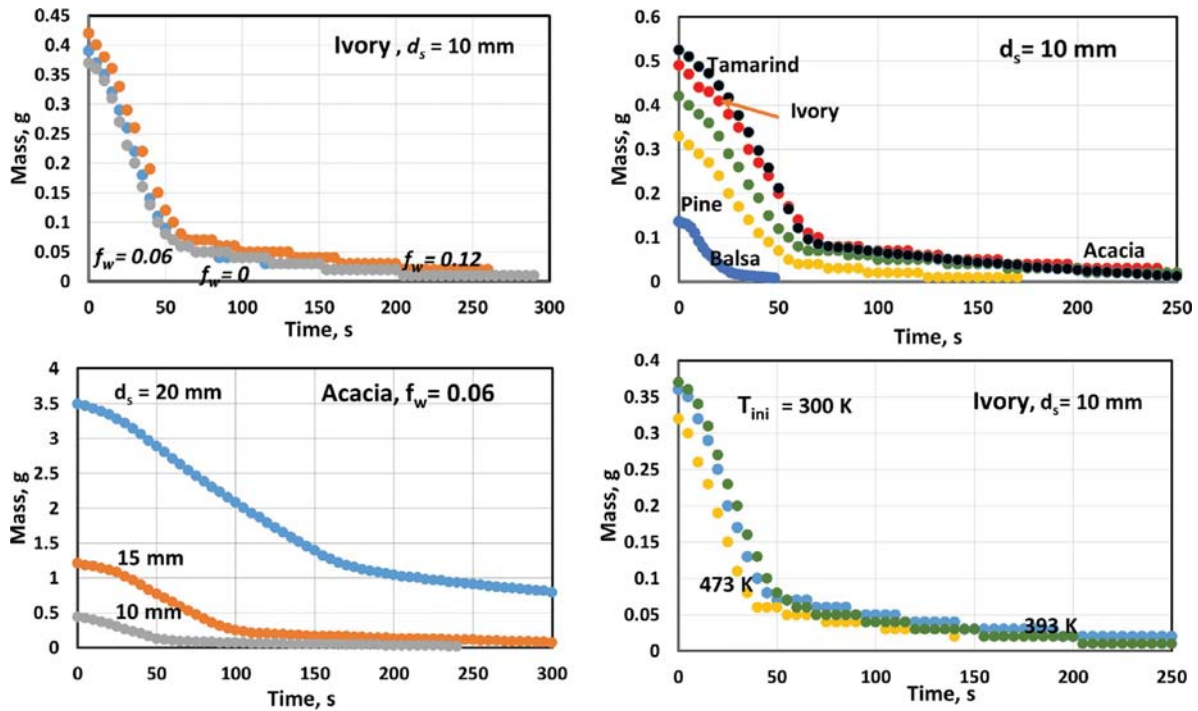


Fig. 4. Select mass vs time plots showing species, size, moisture fraction and initial temperature effects.

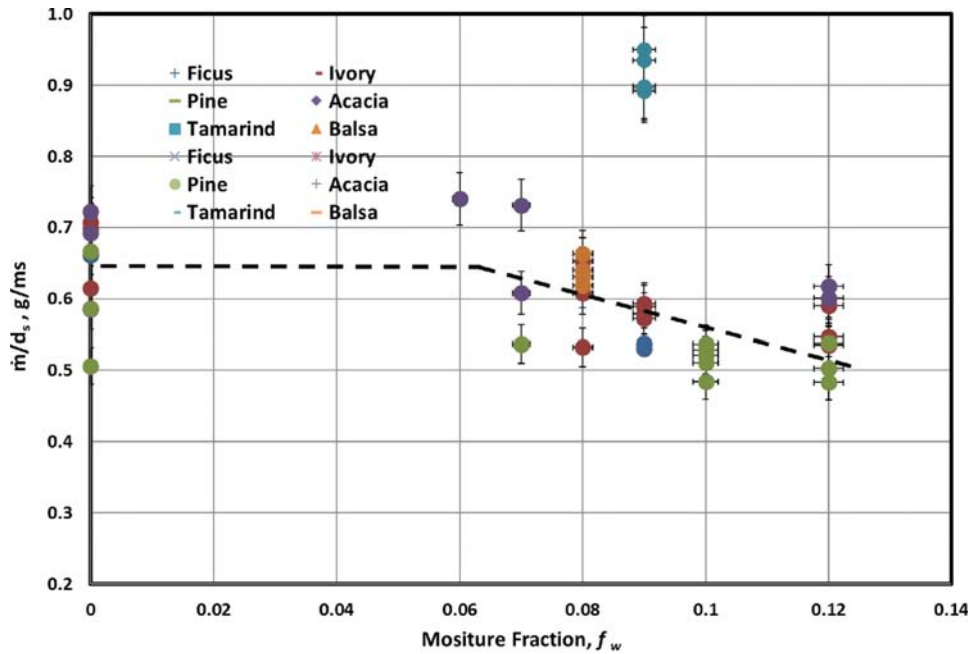


Fig. 5. The ratio of mass burn rate to initial sphere diameter with moisture fraction.

The third important parameter concerns B . Two biomass condensed phase parameters controlling the burn behaviour are the specific heat and the heat of pyrolysis both of which have been discussed in the introduction. Based on these and the discussion to follow, the following expression for B is set out.

$$B = 1.0(1320 - 600)/[H_p + (1.5 + 4f_w)(600 - T_{ini})] \quad (12)$$

In the above equation, c_{pg} is set as 1.0 kJ/kg K, T_f is set as 1320 K (obtained from measurements discussed below) independent of f_w since the role of f_w is perceived partly to be chemical — the inefficiencies in the burning of more tarry compounds is compensated by

less complex composition that emanates from the surface due to steam-char reactions, thus maintaining the flame temperature to be about same. The surface temperature, T_s is set at 600 K for all the situations considered. Its variation is about ± 20 K and is considered small enough to be ignored. The value of H_p is to be treated as a function of biomass. In order to provide a more general treatment and yet not too complex, it is taken as

$$H_p = H_{p0} + 50 [(T_{ini} - 300)/300]^2 + 100(f_w - 0.1) \quad (13)$$

The value of H_{p0} is the heat of pyrolysis of sun-dry biomass (considered as at $f_w = 0.1$) at an ambient temperature of 300 K. It is the parameter

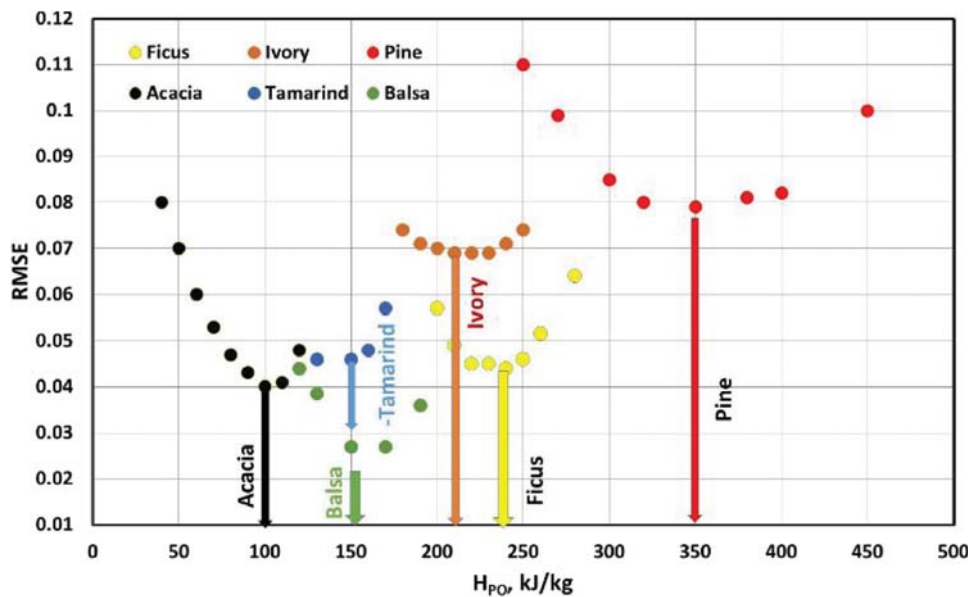


Fig. 6. The variation of the root mean square error, $RMSE$ with the heat of pyrolysis, H_{p0} .

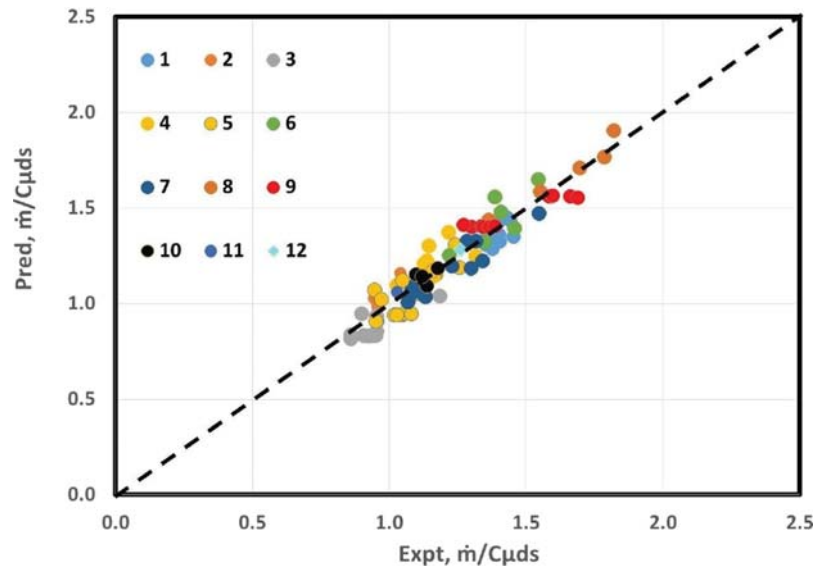


Fig. 7. Predicted vs experimental dimensionless mass burn rate (1- Ficus-Sph-373 to 423 K, 2- Ficus-Sph-300 K, 3-Pine-Sph-300 K, 4-Pine-Sph-393 to 423 K, 5- Ivory-Sph-300 K, 6- Ivory -Sph- 393 to 423 K, 7-Acacia- Sph- 300 K, 8-Acacia- Sph- 393 to 423 K, 9- Tamarind- Sph- 300 K, 10- Balsa- Sph- 300 K, 11- Mahagony- Sph- 300 K, 12- Momeni- Sph).

that depends on the specific biomass. The choice of the values 50 and 100 in the above equation were those arrived at by varying them to provide minimum error in the predicted burn rate in comparison to a large number of experimental data on spheres to be described further. The only parameter specific to the biomass varied to get good fit for the entire range of tests is H_{p0} .

4. The samples and preparation

Six different biomass were used in this study. Ficus (*Ficus Benghalensis*, banyan tree of India), Ivory (*Wrightia tinctoria*, locally called Haale tree), Acacia (*Acacia nilotica*, called babul locally), Pine (*Pinus roxburghii*), Balsa (*Ochroma pyramidale*) and Tamarind (*Tamarindus indica*) spheres were obtained from a wood working toy industry using knot-free wood. While Ficus spheres were all of 15 mm size, other biomass was obtained at diameters of 10, 15 and 20 mm. The samples were subject to proximate and ultimate analysis using standard procedures from an outside laboratory. The results are set out in Table 1. As

can be expected, the ash content of all these tree based samples have a small ash fraction (about or less than a percent). The other fractions are very similar.

Fig. 2 shows the pictures of spheres used in the experiments. The temperature dependence studies involved the first four species. The densities are Ficus $\sim 630 \text{ kg/m}^3$, Ivory ~ 630 to 680 kg/m^3 , Acacia ~ 700 to 750 kg/m^3 , Pine ~ 350 to 500 kg/m^3 , Tamarind ~ 960 to 1016 kg/m^3 , and Balsa ~ 250 to 300 kg/m^3 . Experiments showed that for some samples, the density varied widely. This is considered not unusual and is thought to be related to samples over a cross section, with core showing lower density than from the peripheral region.

In each experiment, the samples were measured and weighed at two stages — before drying or heating and just before the experiment. For the experiments at the ambient temperature ($300 \pm 3 \text{ K}$), the samples were dried in the furnace at a temperature of 378 K for 24 h and their weight was noted after cooling them in a desiccator. They were dried again in the furnace for 8 h, cooled and weighed. If, for a given sample,

Table 2
Mean values of experimental \dot{m}/d_s , \dot{m}_n at various T_{ini} ; $C_\mu = 0.562$ g/m s.

Species	\dot{m}/d_s		\dot{m}_n	
	at 300 K		T_{ini} of 393 – 473 K	
	g/m s	–	g/m s	–
Ficus	0.58	1.03	0.80	1.42
Ivory	0.60	1.06	0.78	1.39
Acacia	0.68	1.22	0.86	1.52
Pine	0.53	0.94	0.65	1.15
Tamarind	0.75	1.34	–	–
Balsa	0.60	1.06	–	–

Table 3
Values of H_{p0} for various species.

Species	Ficus	Ivory	Acacia	Pine	Tamarind	Balsa
H_{p0} , kJ/kg	240	210	100	350	–150	150

Table 4
Comparison of mass loss data of pine sphere (Momeni [32]), E = experiment, P = present correlation, $\rho_{fu} = 600$ kg/m³, $f_w = 0.09$, $T_{ini} = 300$ K, $H_{p0} = 208$ kJ/kg, the symbol “–” means < 5%.

d_s mm	L mm	\dot{m} g/s	\dot{m}_n E	T_{fur} K	B	\dot{m}_n P	–
3.0	3.00	2.1	1.26	2200	1.96	1.28	–

there was no difference between the two weights, it was taken that the sample was dry.

For sun-dry conditions, the dried samples were allowed in the ambient atmosphere to equilibrate for 24 h before the moisture was estimated by drying it and testing it as a procedure. For the experiments with larger moisture content, the samples were fully dried as in the earlier paragraph and then the sample was wrapped in a wet cloth having a moisture fraction a little above the desired value (14% if the desired moisture fraction is 12%). After the sample was kept for four hours, the sample was separated and weighed. If this showed the requisite rise in moisture content, it was immediately taken for the combustion test. The duration of four hours was decided based on studies to ensure that additional duration does not alter the mass of the sample. The moisture fraction is calculated based on the dry weight of the sample. The equivalent diameter obtained here is the average value of the diameter measured in three orthogonal directions.

For experiments at higher temperatures (393, 423 and 473 K), the samples were kept in the furnace at the required temperature for 24 h and experiments were conducted immediately after the sample was removed from the furnace.

5. The experimental arrangement and procedure

Fig. 3 shows the experimental arrangement to obtain the mass loss and gas phase temperature data and the photograph of the burning wood sphere. The sphere was mounted with the aid of a stand and needle arrangement and it was placed on an electronic mass balance of the least count 0.1 mg. The data on mass was taken to a computer through an RS232 interface. The sphere mounting arrangement and the mass balance were separated by means of alumino-silicate blanket of 15 mm thickness. During the days experiments were conducted the ambient temperature was 300 ± 3 K and the relative humidity was measured as $55 \pm 5\%$.

Before starting the experiment, the sample mounted on the needle was sprayed with small amount of diesel fuel and it was ignited by means of a spirit lamp till 10% of weight loss of the samples, so that the sample stands ignited even with more difficult experimental conditions like those at 10% moisture. The mass loss of the sample was continuously measured during the burn. The time when the wood sample is fully ignited and achieves steady burn takes about 5 to 15

s. A thermocouple of 0.1 mm bead size is used to obtain the flame temperature, T_f . The thermocouple was introduced into the flame and gently moved around to obtain the peak temperature. The measured value of T_f was between 1300 K to 1340 K. A mean value of 1320 K has been set for T_f .

6. Results and discussion

After several preliminary studies, 90 experiments with more than 15 for each of the species were conducted. At least two experiments at each condition were conducted. Fig. 4 shows typical mass vs time for several representative cases considered here. The plot at the left hand top shows the influence of moisture fraction on the mass vs time curve for 10 mm diameter of Ivory. The effect on the burn time is small. The plot on the bottom left shows the effect of sphere diameter and the mass loss vs time curves are significantly spaced indicating the strong dependence of burn time on diameter. The top right plot shows the role of the specific biomass of the same diameter on the mass vs. time behaviour. The initial mass is different because of the density of the biomass. The lightest of the biomass tested, namely, balsa has a flaming time on the order of 35 s and highest density biomass, Tamarind has a flaming time of 75 s. The bottom right plot shows the effect of initial temperature with sphere of ivory at 10 mm diameter. The effect on the flaming time is not significant. As can be noted, many curves have a near-linear variation of mass vs time over the flaming period. *The slope constitutes the mass burn rate of the specific case.* As can be noticed, the linear variation after a short transient is present for all the biomass over a range of densities from 250 to 1000 kg/m³.

The ratio of the mass burn rate with initial diameter, \dot{m}/d_s from the experiments for different moisture fractions, f_w at $T_{ini} = 300$ K is set out in Fig. 5. As can be noted, there is sufficient variation (not scatter) between different biomass at each moisture fraction and there is a tendency for the mass burn rate to go down with moisture fraction. This is particularly so when 12% moisture is reached. Also \dot{m}/d_s varies from about 0.5 to 0.9 g/m s over different biomass and moisture fractions up to 0.12.

The mean results of the burn rate data at 300 K (7 to 12% moisture fraction) as well as at higher temperatures of 393 K, 423 K and 473 K are set out in Table 2. Across the species, there is a clear 25% variation in the burn rate and with enhanced initial temperature, the burn flux increase for each species can up by 35% from the values at ambient conditions. The largest contributor to this change is the change in B . Also, Tamarind burns the fastest while Pine, the lowest. These results are interesting and new.

The entire data set was classified according to species, moisture fraction and initial temperature. The prediction used essentially the Eqs. (11), (12) and (13). Optimization effort consisted in minimizing the root mean square error between the predicted and the experimental values of $\dot{m}/C_\mu d_s$ for each species. The root mean square error, $RMSE$ is defined by

$$RMSE = \sqrt{\sum_{i=1}^{noe} [(\dot{m}_n, E - \dot{m}_n, P) / \dot{m}_n, E]^2} \quad (14)$$

where noe is the number of experiments for each of the samples that was 14 for Ficus, 21 for Ivory, 20 for Pine, 17 for Acacia, 11 for Tamarind and 4 for Balsa. The averages were obtained by making a choice of the heat of pyrolysis defined in Eq. (13). The results of the calculations are set out in Fig. 6.

This figure is revealing. As one varies the choice of H_{p0} for each of the sets, the error goes through a minimum as may be expected. But the nature of variation is different in the case of Ivory for which the variation is flat where as with others it is sharp. The values of H_{p0} are chosen at the lowest of RMSE for each species. The values are set out in Table 3.

The values differ significantly over the species. These values are connected to the combustion process directly because they are deduced from the expectation of predicting the burn rate of biomass (spheres

Table 5

Comparison of mass loss data of spheres at $T_{ini} = 300$ K, E = experiment, P = predicted, the symbol “-” means $< 5\%$, $C_{\mu} = 0.562$ g/m s.

Species	d_s mm	f_w %	ρ_{fs} kg/m ³	\dot{m} mg/s	\dot{m}_n E	H_{p0} kJ/kg	B	\dot{m}_n P	Error %
Ficus	15.7	0	639	9.2	1.04	240	1.06	1.16	+11
	15.6	0	711	10.3	1.18		1.06	1.15	-
	15.4	0.10	622	8.2	0.94		0.90	1.03	+9
	15.2	0.10	643	8.2	0.96		0.86	0.98	-
Ivory	10.1	0	690	6.2	1.09	210	1.11	1.05	-
	10.3	0.08	702	6.0	1.03		0.94	0.94	+11
	10.4	0.12	701	5.6	0.95		0.89	0.91	-
	10.3	0.09	690	6.1	1.04		0.94	0.94	-10
	15.3	0	640	10.8	1.26		1.11	1.19	-
	15.6	0.08	650	8.3	0.95		0.96	1.07	+13
	15.5	0.12	650	8.5	0.96		0.89	1.02	-
	20.4	0	667	14.2	1.24		1.11	1.31	-
	20.3	0.08	710	13.3	1.15		0.96	1.17	-
	20.3	0.12	663	12.0	1.04		0.89	1.13	+6
Acacia	10.1	0	682	7.0	1.23	100	1.33	1.19	-
	10.2	0.07	792	6.2	1.08		1.14	1.06	-
	10.6	0.12	775	6.4	1.07		1.03	1.01	+6
	10.2	0.09	796	6.5	1.13		1.10	1.04	-8
	10.5	0.09	751	6.4	1.08		1.10	1.05	-
	14.7	0	661	10.6	1.29		1.33	1.33	-
	14.7	0.07	728	10.8	1.30		1.14	1.18	-9
	14.6	0.12	715	9.0	1.10		1.04	1.11	-
	19.7	0	654	17.2	1.55		1.33	1.47	-
	20.0	0.06	834	14.8	1.32		1.17	1.33	-
	19.9	0.12	765	15.0	1.34		1.03	1.22	-8
Pine	10.3	0	475	5.2	0.90	350	0.91	0.95	-
	10.1	0.07	556	5.4	0.95		0.82	0.86	-10
	10.3	0.12	568	5.0	0.86		0.76	0.81	-
	10.3	0.10	520	5.0	0.86		0.78	0.84	-
	14.5	0	484	9.7	1.19		0.91	1.04	+12
	14.6	0.10	455	7.8	0.95		0.78	0.93	-
	14.9	0.12	518	8.0	0.96		0.76	0.91	-
	18.2	0	463	10.7	1.04		0.91	1.13	+8
	18.3	0.12	446	9.2	0.89		0.76	0.99	+10
Tamarind	10.0	0.09	992	7.3	1.30	-150	1.77	1.40	-
	10.2	0.09	961	7.3	1.27		1.77	1.41	+10
	10.0	0.09	970	7.5	1.33		1.77	1.40	-
	10.0	0.09	1007	7.5	1.34		1.77	1.40	-
	10.1	0.09	992	7.8	1.38		1.77	1.40	-
	10.0	0.09	1016	7.6	1.36		1.77	1.40	-
	14.8	0.09	988	13.8	1.66		1.77	1.56	-6
	14.7	0.09	1033	13.9	1.69		1.77	1.55	-8
	14.7	0.09	996	13.2	1.59		1.77	1.56	-
	14.7	0.09	977	13.1	1.58		1.77	1.56	-
	14.8	0.09	972	13.3	1.59		1.77	1.56	-
Balsa	9.6	0.08	299	6.2	1.13	150	1.04	1.09	-
	10.5	0.08	225	7.0	1.18		1.04	1.18	-
	10.3	0.08	248	6.4	1.10		1.04	1.15	-
	10.3	0.08	262	6.5	1.12		1.04	1.14	-

here). It can be seen that most of the species show endothermic values for the heat of pyrolysis. It must be emphasized that this approach to the determination of the heat of pyrolysis and the transfer number (to be discussed later) provides definitive estimation of these parameters.

The predictions and the experimental data for spheres are set out in the Appendix as Tables 5 and 6. These tables present the data on their diameter, moisture fraction, initial temperature at which the samples were conditioned, the density of the sphere, mass burn rate, dimensionless mass burn rate, the value of H_{p0} , the transfer number, B obtained from this correlation and the predicted dimensionless burn rate with the last column indicating the percentage error in the predictions for tests at ambient temperature and higher initial temperatures respectively. Those with errors less than 5% have been considered very good predictions since the accuracy of the burn rate data is limited to this value.

It can be noted that B is about 1 for Ficus, Ivory and Balsa, 0.8 to 0.9 for Pine, 1.1 to 1.3 for Acacia and 1.8 for Tamarind at an ambient temperature of 300 K. For higher temperatures, the values are larger

going up to 2.4. The burn rate predictions using Eqs. (11) to (13) seem to be good over the range of conditions considered.

6.1. Comparison with the experiments of Momeni et al. [32]

Momeni et al. [32] conducted combustion like experiments with pine spheres and cylinders of small diameter different aspect ratio, but all with nearly same volume. The samples were burnt in an atmosphere of the combustion products of a fuel gas, presumably natural gas at near-stoichiometric conditions. The measured temperature and oxygen fraction of the hot gases are 1673 K and 0.03 to 0.04. While their experiments have dealt with ignition and char burn out conditions as well, the data of interest here is in volatile combustion rate. They have provided data on the time for conversion of various phases. They report a value of density of 600 kg/m³ and use of this value leads to mass that are lower than indicated. Specifically, they indicate a mass of 0.0125 g, but the mass obtained with the density provided leads to a mass of 0.0085 g. Thus the value of 0.0085 g is retained in the

Table 6

Comparison of mass loss data of spheres at higher initial temperatures, $f_{w0} = 0$, E = experiment, P = predicted, the symbol “-” means < 5%.

Species	d_s mm	T_{ini} %	ρ_{fa} K	\dot{m} kg/m ³	\dot{m}_n E mg/s	H_{p0}	B kJ/kg	\dot{m}_n P	Error %
Ficus	15.2	393	702	12.0	1.40	240	1.32	1.33	-
	15.6	393	659	12.0	1.37		1.32	1.34	-
	16.1	423	636	13.0	1.44		1.43	1.43	-
	15.9	423	607	12.5	1.40		1.43	1.43	-
	15.0	373	630	11.6	1.38		1.26	1.29	-6
	15.6	373	590	11.8	1.35		1.26	1.31	-
	15.9	393	673	13.0	1.45		1.32	1.35	-7
	16.0	393	560	12.2	1.36		1.32	1.37	-
	15.8	393	600	12.5	1.40		1.32	1.36	-
Ivory	10.4	393	611	7.1	1.22	210	1.40	1.25	-
	10.6	423	641	8.0	1.34		1.52	1.32	-
	15.3	393	621	12.4	1.46		1.40	1.39	-
	16.0	393	620	12.3	1.36		1.40	1.41	-
	15.5	423	594	12.1	1.41		1.52	1.48	-
	20.8	393	606	16.2	1.39		1.40	1.56	+12
	20.9	423	612	18.2	1.54		1.52	1.65	+6
Acacia	10.2	393	718	7.4	1.36	100	1.78	1.44	+10
	9.8	473	790	9.4	1.70		2.42	1.71	-
	14.5	393	708	12.7	1.55		1.78	1.59	-
	19.9	393	726	20.0	1.79		1.78	1.77	-
	19.9	423	633	20.4	1.82		1.98	1.91	-
Pine	10.4	393	441	6.0	1.03	350	1.10	1.09	+6
	10.4	423	492	7.0	1.16		1.17	1.14	-
	14.8	393	443	9.5	1.13		1.10	1.21	+7
	15.1	393	414	9.6	1.14		1.10	1.22	+7
	14.5	423	476	10.8	1.32		1.17	1.25	-6
	18.12	393	475	12.2	1.15		1.10	1.30	+13
	18.11	423	460	13.0	1.22		1.17	1.37	+12

analysis to follow. The scatter in the data for some cases where they have done multiple experiments is about 10%. The predictions made here assume a flame temperature of 2200 K taking note of the fact that there is residual oxygen in the high temperature stream. The prediction procedure is the same as discussed earlier and Table 4 shows the details of the comparison of the results.

7. Procedure to estimate B for biomass

Biomass spheres of suitable dimensions, typically of 10 mm diameter should be produced in numbers. Samples drawn from these are conditioned at moisture levels, and dry samples should be conditioned at 0% moisture and also at temperatures up to 423 K or thereabouts to ensure there is no loss of mass during the conditioning. The samples can then be drawn and subject to combustion experiments and the mass loss histories obtained. These are subjected to an analysis to obtain the value of H_{p0} minimizing the error in the prediction of mass loss rate. This process also gives the value of B at ambient temperature albeit within an error band. The mean value will then be the B for the tested biomass. Using this values of B the results of calculations over the full data is obtained set out in terms of predicted vs experimental \dot{m}_n as in Fig. 7. As can be noted, the dimensionless correlation seems to work very well.

8. Concluding remarks

In the present study, experiments on the combustion of biomass spheres of six different species and three different sizes have been conducted at various conditions of moisture fraction and for dried samples, at various conditioning temperatures below the pyrolysis temperature to evaluate the burn rate behaviour and examine the possibility of extracting the transfer number B . Noting various dependences with (a) the dependence of the heat of pyrolysis on the species, and (b) the role of shrinkage influencing the effective diameter for combustion, a model was set out to describe the burn behaviour in a dimensionless format.

The final correlation predicts the burn rate of all the dependences within a root mean square error of less than 5%. The comparison of the predictions from the correlation with the experiments of earlier researchers and those from present experiments appears to be good.

An approach to determining the transfer number for each biomass species through the conduct of burn rate experiments on the 10 mm diameter spheres has been suggested. This procedure gives an opportunity to classify biomass like liquid fuels which have been long characterized using the transfer number.

The value of B is about 1 for Ficus, Ivory and Balsa, 0.8 to 0.9 for Pine, 1.1 to 1.3 for Acacia and 1.8 for Tamarind at an ambient temperature of 300 K. It may be noted that this is new finding in the field of biomass combustion behaviour. The fact that the mass flux is species-dependent brings forth the need for standardization in crib fire studies relevant to fire safety testing.

Data availability

Data will be made available on request.

Acknowledgments

The authors are thankful to the authorities of Jain (Deemed-to-be-university) for encouragement in the conduct of this research.

Appendix

See Tables 5 and 6.

References

- [1] K.W. Ragland, D.J. Aerts, Properties of wood for combustion analysis, *Bioresource Technol.* (37) (1991) 161–168.
- [2] E.R. Huff, Effect of size, shape, density, moisture and furnace wall temperature on burning times of wood pieces, *Fund. Thermochem. Biomass Convers.* (1985) 761–775.

- [3] K.L. Friquin, Material properties and external factors in influencing the charring rate of solid wood and flue laminated timber, *Fire Mater.* (35) (2011) 303–327.
- [4] P.S. Maa, R.C. Bailie, Influence of particle sizes and environmental conditions on high temperature pyrolysis of cellulosic material - I (theoretical), *Combust. Sci. Technol.* (7) (1973) 257–269.
- [5] D.L. Pyle, C.A. Zaror, Heat transfer and kinetics in the low temperature pyrolysis of solids, *Chem. Engg. Sci.* (39) (1984) 147–158.
- [6] C. di Blasi, Heat momentum and mass transport through a shrinking biomass particle exposed to thermal radiation, *Chem. Eng. Sci.* (51) (1996) 1121–1132, 1996.
- [7] I. Glassman, *Combustion*, second ed., Academic Press, 1987.
- [8] A.I. Bartlett, R.M. Hadden, L.A. Bisby, A review of factors affecting the burning behaviour of wood for application to tall building construction, *Fire Technol.* (55) (2018) 1–49.
- [9] E.R. Tinney, The combustion of wooden dowels in heated air, in: Tenth Symposium (International) on Combustion, 1965, pp. 925–930.
- [10] R. Capart, L. Falk, M. Gelus, Pyrolysis of wood macro-cylinders under pressure: Application of a simple mathematical model, *Appl. Energy* (30) (1988) 1–13.
- [11] J. de Ris, A.M. Kanury, M.C. Yeun, Pressure modeling of fires, in: Thirteenth Symposium (International) on Combustion, 1973, pp. 1033–1038.
- [12] H. Lu, W. Robert, G. Pierce, B. Ripa, L.L. Baxter, Comprehensive study of biomass particle combustion, *Energy Fuels* (22) (2008) 2826–2839.
- [13] H. Lu, Ip. Elvin J. Scott, P. Foster, M. Vickers, L.L. Baxter, Effect of particle shape and size on devolatilization of biomass particle, *Fuel* (89) (2010) 1156–1168.
- [14] P.L. Blackshear Jr., A.M. Kanury, Heat and mass transfer to, from, and with cellulosic solids burning in air, in: Tenth Symposium (International) on Combustion, 1965, pp. 911–923.
- [15] L. Orloff, J. de Ris, Modeling of ceiling fires, in: Twelfth Symposium (International) on Combustion, 1971, pp. 979–992.
- [16] C. Dupont, R. Chiriac, G. Gauthier, F. Toche, Heat capacity measurements of various biomass types and pyrolysis residues, *Fuel* (115) (2014) 644–651.
- [17] K. Radmanovic, I. Dukic, S. Pervan, Specific heat capacity of wood - a review, *Drvna Industrija.* (2) (2014) 151–157.
- [18] A.F. Roberts, The heat of reaction during pyrolysis of wood, *Combust. Flame.* (17) (1971) 79–86.
- [19] A.F. Roberts, Problems associated with the theoretical analysis of the burning of wood, in: Ninth Symposium (International) on Combustion, 1971, pp. 893–901.
- [20] I. Milaosavljevic, V. Oja, E.M. Suuberg, Thermal effects in cellulosic pyrolysis: relationship to char forming processes, *Ind. Eng. Chem. Res.* (35) (1996) 653–662.
- [21] A.F. Roberts, G. Clough, Thermal decomposition of wood in an inert atmosphere, in: Ninth Symposium (International) on Combustion, the Combust. Inst, 1963, pp. 158–166.
- [22] H.C. Kung, A.S. Kalekar, On the heat of reaction of wood pyrolysis, *Combust. Flame* (20) (1973) 91–103.
- [23] J.T. Kuo, L.H. Hwang, Mass and thermal analysis of burning wood spheres, *Combust. Sci. Technol.* (175) (2003) 665–693.
- [24] H.S. Mukunda, P.J. Paul, U. Shrinivasa, N.K.S. Rajan, Combustion of wooden spheres- experiments and model analysis, in: Twentieth Symposium (International) on Combustion, the Combust. Inst, 1984, pp. 1619–1628.
- [25] G.A. Agoston, H. Wise, W.A. Rosser, Dynamic factors affecting the combustion of liquid spheres, in: Sixth Symposium (International) on Combustion, 1957, pp. 708–717.
- [26] H.R. Baum, A. Atreya, A model for combustion of firebrands of various shapes, *Fire Saf. Sci.* (11) (2014) 1353–1367.
- [27] H.S. Mukunda, Variable property analysis - is there anything to it, *Sadhana*, (parts 1 and 2), 1988, pp. 187–199.
- [28] B.N. Raghunandan, H.S. Mukunda, The problem of liquid droplet combustion - a reexamination, *Combust. Flame.* (30) (1977) 71–84.
- [29] G.A. Agoston, B.J. Wood, H. Wise, Influence of pressure on the combustion of liquid spheres, *Jet Propul.* (1985) (1958) 181–188.
- [30] M.R. Barr, R. Jervis, Y. Zhang, A.J. Bodey, C. Rau, P.R. Shearing, D.J.L. Brett, M.M. Titrici, R. Volpe, Towards a mechanistic understanding of particle shrinkage during biomass pyrolysis via synchrotron X-ray microtomography and in-situ radiography, *Nat. Sci. Rep.* (11) (2021) 26–56.
- [31] Q.X. Huang, R.P. Wang, W.J. Li, Y.J. Tang, Y. Chi, J. Yan, J. H, Modelling and experimental studies of the effects of volume shrinkage on the pyrolysis of waste wood sphere, *Energy Fuels* (28) (2014) 6398–6406.
- [32] M. Momeni, C. Yin, S.K. Kaer, T.B. Hansen, P.A. Jensen, P. Glarborg, Experimental study on effects of particle shape and operating conditions on combustion characteristics of single biomass particles, *Energy Fuels* (27) (2013) 507–514.